

AuPd/3DOM TiO₂ Catalysts: Good Activity and Stability for the Oxidation of Trichloroethylene

Xing Zhang, Yuxi Liu, Jiguang Deng, Kunfeng Zhang, Jun Yang, Zhuo Han and Hongxing Dai *

Beijing Key Laboratory for Green Catalysis and Separation, Key Laboratory of Beijing on Regional Air Pollution Control, Key Laboratory of Advanced Functional Materials, Education Ministry of China, Laboratory of Catalysis Chemistry and Nanoscience, Department of Chemistry and Chemical Engineering, College of Environmental and Energy Engineering, Beijing University of Technology, Beijing 100124, China; xingz@emails.bjut.edu.cn (X.Z.); yxliu@bjut.edu.cn (Y.L.); jgdeng@bjut.edu.cn (J.D.); kfzhang@emails.bjut.edu.cn (K.Z.); yangjun123@emails.bjut.edu.cn (J.Y.); hz102938@emails.bjut.edu.cn (Z.H.)

* Correspondence: hxdai@bjut.edu.cn; Tel.: +8610-6739-6118; Fax: +8610-6739-1983

Content

Item	Page
Catalyst characterization procedures	3-5
Figure S1	8
Scheme S1	9
Scheme S2	10
Figure S2	11
Figure S3	12
Table S1	13-14
Figure S4	15
Table S2	16

Catalyst characterization procedures:

The actual Au_yPd contents in the xAu_yPd/3DOM TiO₂ (*x* is the loading (wt%) of Au_yPd NPs, and *y* is the molar ratio of Au/Pd) samples were measured using the inductively coupled plasma–atomic emission spectroscopic (ICP–AES) technique on a Thermo Electron IRIS Intrepid ER/S spectrometer. Each sample was dissolved in a mixture of concentrated HCl and HNO₃ aqueous solutions with a volumetric ratio of 3.0 : 1.0 prior to analysis.

The crystal phase compositions of the samples were determined by means of X-ray diffraction (XRD) on a Bruker D8 Advance diffractometer with Cu K α radiation and nickel filter ($\lambda = 0.15406$ nm), The data were collected at scattering angles (2θ) from 10 to 80 °.

Scanning electron microscopic (SEM) images of the samples were recorded on a Gemini Zeiss Supra 55 apparatus (operating at 10 kV). High-resolution transmission electron microscopic (HRTEM) images of the samples were obtained using the JEOL-2010 equipment (operating at 200 kV). High angle annular dark field and scanning transmission electron microscopic (HAADF–STEM) images and element mapping were acquired on the equipment FEI G2 80–200/Chemi–STEM Cs-corrected transmission electron TEM with probe corrector.

Specific surface areas and pore sizes of the samples were determined on a Micromeritics ASAP 2020 instrument via N₂ adsorption at –196 °C with the sample being degassed under vacuum at 300 °C for 2 h before measurement, and calculated using the Brunauer–Emmett–Teller (BET) and Barrett–Joyner–Halenda (BJH) methods, respectively.

X-ray photoelectron spectroscopy (XPS) was used to measure the Ti 2p, O 1s, Au 4f, Pd 3d, and C 1s binding energies (BEs) of surface species using Mg K α ($h\nu = 1253.6$ eV) as excitation source. In order to remove the adsorbed water and carbonate species on the surface, the samples were pretreated in O₂ (flow rate = 20 mL/min) at 400 °C for 1 h and then cooled to room temperature, followed by transferring the pretreated samples into the spectrometer in a transparent Glove Bag (Instruments for Research and Industry, USA) that was filled with helium. The pretreated samples were outgassed in the preparation chamber (10^{–5} Torr) for 0.5 h and then introduced into the analysis chamber (3 × 10^{–9} Torr) for XPS spectrum recording.

A range of background (BG) types are offered, the most commonly used types are linear, Shirley and Tougaard. Linear backgrounds are typically used for insulating materials, while steps in metallic data are modeled using the Shirley BG. The full set of BG types can be selected via a dialog window invoked by holding the control key down and left-clicking over the current BG-type setting before the parameter is an edit field. In the present work, we use the Shirley BG. The charging effects were corrected with respect to C 1s (binding energy = 284.6 eV). Atomic ratios of surface elements were calculated after correcting the XPS signal intensity using atomic sensitivity factors.

The CasaXPS (computer aided surface analysis for X-ray photoelectron spectroscopy) software was used to perform carbon calibration and peak fitting of the data. CasaXPS is a computer program that allows to process the XPS data. It offers a powerful data processing environment on a PC. It can do angle-resolved and depth profile XPS. The best route to create quantification regions is via the element library dialog window. The advantage of using the element library lies in the direct link between specifying the peaks and the RSF scaling information from the library. The simplest route to creating quantification regions is via the Find Peak/Create Region buttons on the element table property page. Using the element library dialog window, the first step is therefore to enable element markers for all the appropriate species within the data. The manual route to enabling element markers involves the element table, the left-hand pane and the mouse. With the Element Table property page topmost on the element library dialog window, left-click the mouse with the cursor pointing at a peak in the data. The element table scrolls to display those transitions with energies around the energy indicated by the mouse. Select the most likely transition from the table on the Element Table using the name field. Element markers are placed on the data for all transitions in the element table from the indicated element. The process is repeated for each peak in the data until all peaks are assigned to element markers. Regions are created based on the proximity of element markers to the peaks in the data. In the event the energy scale needs calibrating, the calibration step

should be performed before attempting to create regions. To calibrate the energy scale for an individual C 1s spectrum. Press the Apply button to calibrate the spectrum in the active tile. Provided the peaks are within a tolerance of the element markers and the peaks of interest are accounted for by the element markers, pressing the Create Region button on the Element Table property page will create a set of regions on the spectrum. An annotation table offering a quantification table is added to the spectrum. If the Regions property page on the quantification parameter dialog window is top-most, stepping through the set of regions using the zoom options allows the limits for the regions to be visually inspected and adjusted under mouse control.

The full width at half maximum (FWHM) are useful indicators of chemical state changes and physical influences. A set of relative sensitivity factors are necessary for transitions within an element and also for all elements, where the sensitivity factors are designed to scale the measured areas so that meaningful atomic concentrations can be obtained, regardless of the peak chosen. In principle, the peak intensity measures how much of a material is at the surface, the peak positions in terms of binding energy provide information about the chemical state for a material. The diameter of the analyzer, the pass energy and the spread of energies in the X-ray source play a major role in determining the full width half maximum (FWHM) for a given photoelectric line. In the present work, the asymmetric O 1s XPS signal could be decomposed to three components at binding energy (BE) = 529.6, 531.7, and 533.3 eV (Figure 5A), ascribable to the surface lattice oxygen (O_{latt}), adsorbed oxygen (O_{ads} , e.g., O_2^- , O_2^{2-} or O^-), and carbonate or adsorbed water species. The BEs of Ti 2p_{1/2} and Ti 2p_{3/2} of TiO₂ were 464.1 and 458.3 eV. The two components at BE = 83.4 and 87.3 eV were assigned to the surface Au⁰ species, while the other four components at BE = 84.3, 85.8, 88.4, and 89.9 eV were attributed to the surface Au^{δ+} species. The two components at BE = 335.5 and 340.7 eV were ascribed to the surface Pd⁰ species, whereas the other two components at BE = 337.8 and 342.7 eV were attributed to the surface Pd²⁺ species.

Hydrogen temperature-programmed reduction (H₂-TPR) experiments were carried out on a chemical adsorption analyzer (Autochem II 2920, Micromeritics) equipped with a custom-made thermal conductivity detector (TCD). In each measurement, 30 mg of the sample was first pretreated in a N₂ flow of 30 mL/min at 300 °C for 1 h and then cooled to RT for the removal of the adsorbed CO₂ and H₂O. The sample was then subjected to a 10 vol% H₂-90 vol% Ar flow of 30 mL/min and heated at a ramp of 10 °C/min from RT to 700 °C. The alteration in H₂ concentration of the effluent was monitored online by the chemical adsorption analyzer. The reduction peak was calibrated against that of the complete reduction of a known standard powered CuO (Aldrich, 99.995%) sample.

Oxygen temperature-programmed desorption (O₂-TPD) was carried out on the apparatus same as that in the H₂-TPR experiments. Prior to each test, 50 mg of the sample was preheated in a O₂ flow of 30 mL/min at 300 °C for 1 h to removed the adsorbed CO₂ and H₂O. After being cooled to RT, the sample was heated from RT to 900 °C at a ramp of 10 °C/min in a He flow of 30 mL/min. The oxygen concentration in the effluent was continuously monitored by a thermal conductivity detector. There were several tiny peaks assignable to the background noises.

NH₃ temperature-programmed desorption (NH₃-TPD) was performed in a quartz fixed-bed microreactor on a chemical adsorption analyzer (Autochem II 2920, Micromeritics) equipped with a TCD. 50 mg of the sample was pretreated in a N₂ flow of 20 mL/min at 300 °C for 1 h. After being cooled to 50 °C, the sample was exposed to a NH₃ flow of 20 mL/min for 0.5 h, and then switched to a N₂ flow of 20 mL/min for 1 h for the removal of the physically adsorbed NH₃. Finally, NH₃ desorption took place at a ramp of 10 °C/min from 100 to 900 °C.

In-situ diffuse reflectance Fourier transform infrared spectroscopic (DRIFT) experiments were carried on a Bruker Tensor II spectrometer with a liquid nitrogen-cooling MCT detector. Before the *in-situ* DRIFT experiment, 30 mg of the sample was loaded onto a high-temperature IR cell with ZnSe windows, and preheated in an O₂ flow of 30 mL/min at 300 °C for 1 h. Subsequently, the sample was cooled to RT and purged with a N₂ flow of 30 mL/min for 30 min, and then the background spectrum was recorded at different temperatures. Finally, the sample was kept in a reactant mixture flow (10.0 mL/min) of 750 ppm TCE + 20 vol% O₂ + 80.0 vol% N₂, and the DRIFT

spectra of the samples in the temperature range of 100–450 °C were recorded by accumulating 32 scans at a spectrum resolution of 4 cm⁻¹.

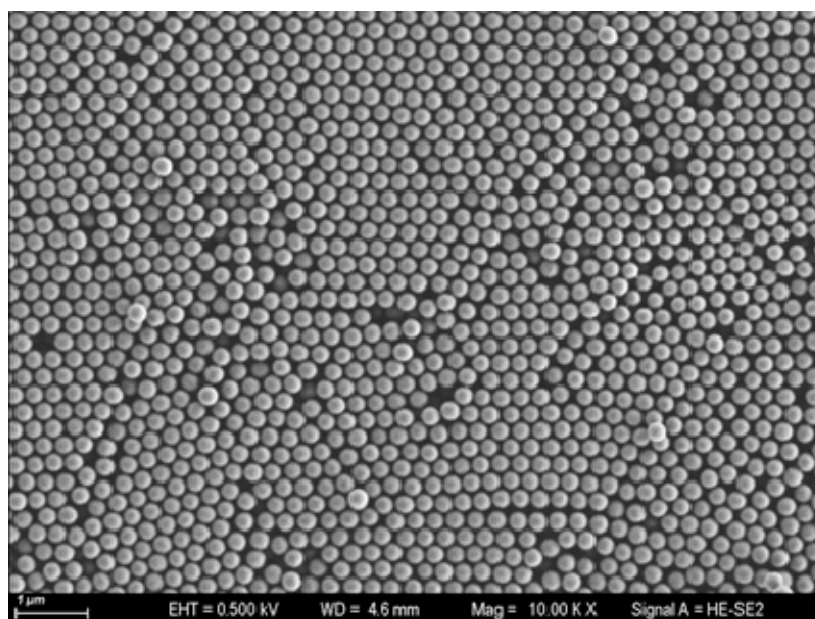
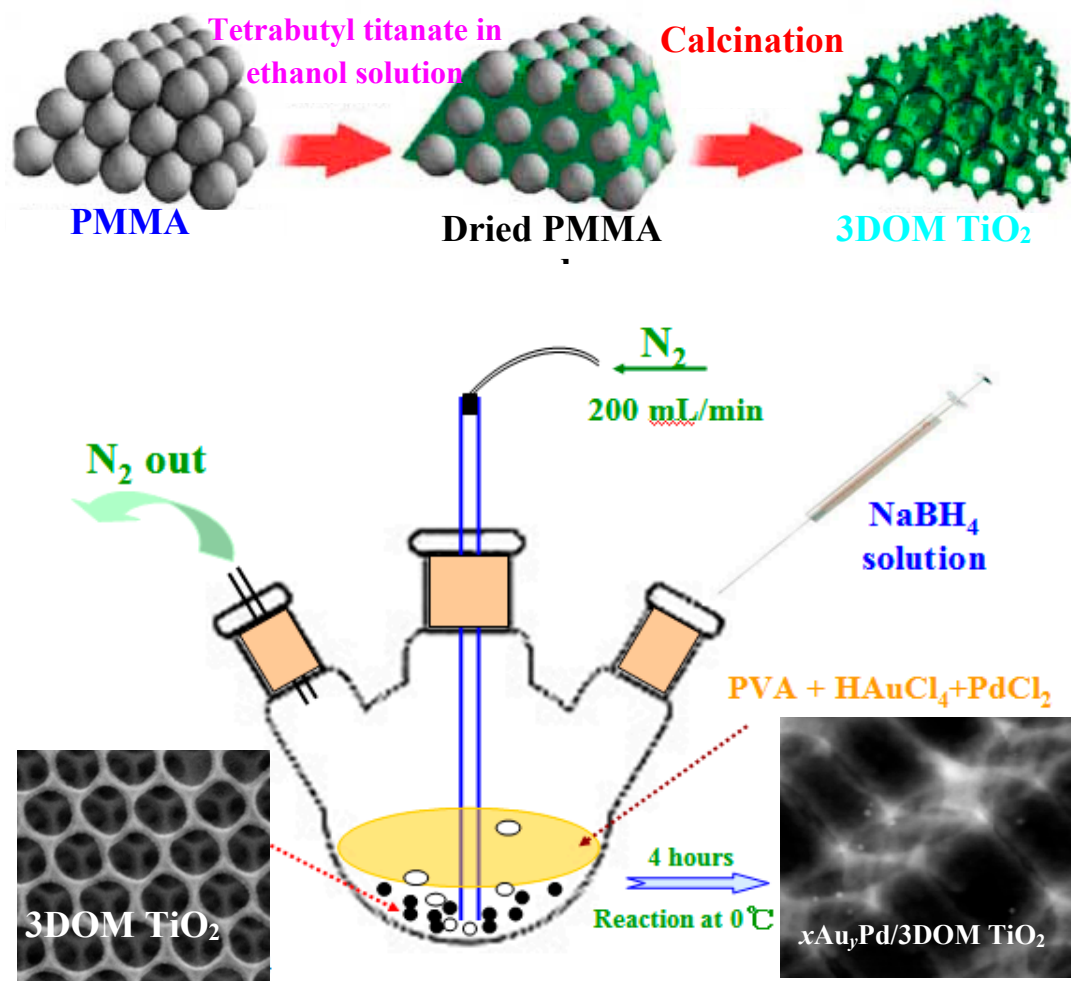
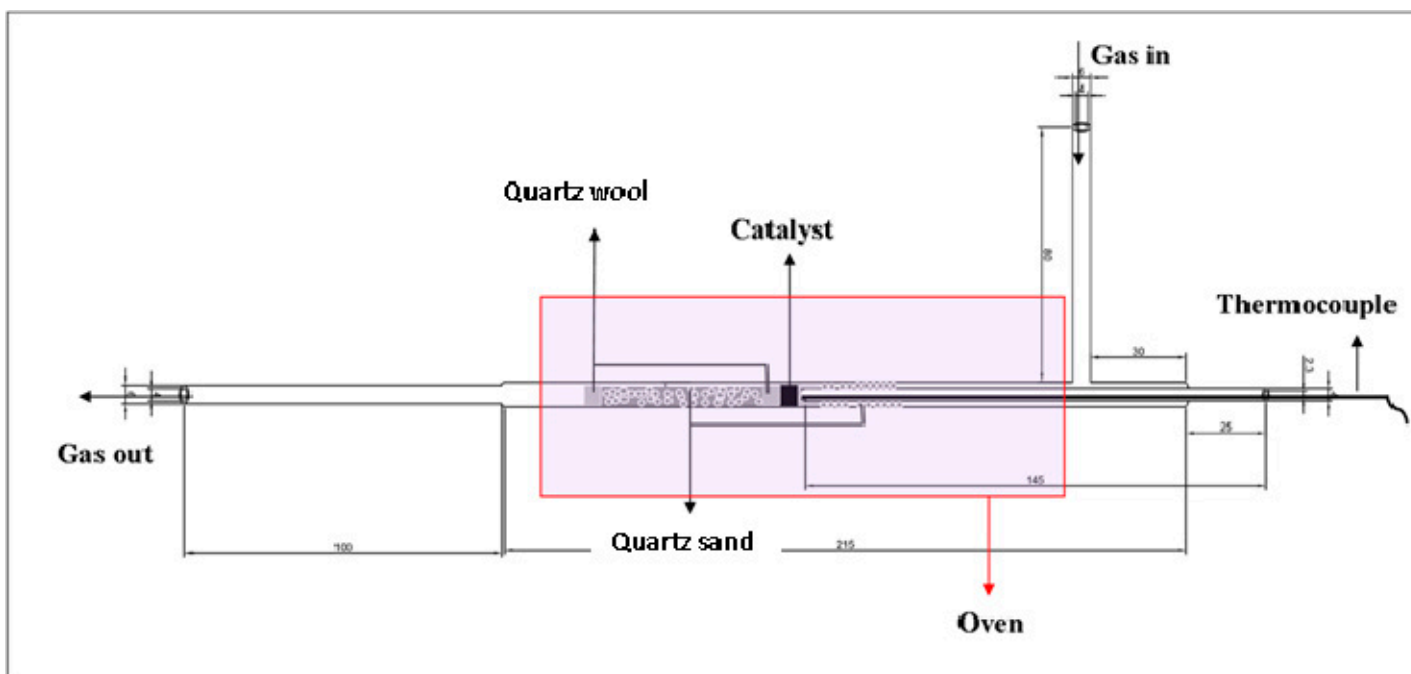


Figure S1. SEM image of the well-aligned PMMA microspheres.



Scheme S1. An illustration for the preparation of the 3DOM TiO₂ and its supported Au-Pd alloy samples.



Scheme S2. An illustration of the quartz tubular microreactor for catalytic activity evaluation.

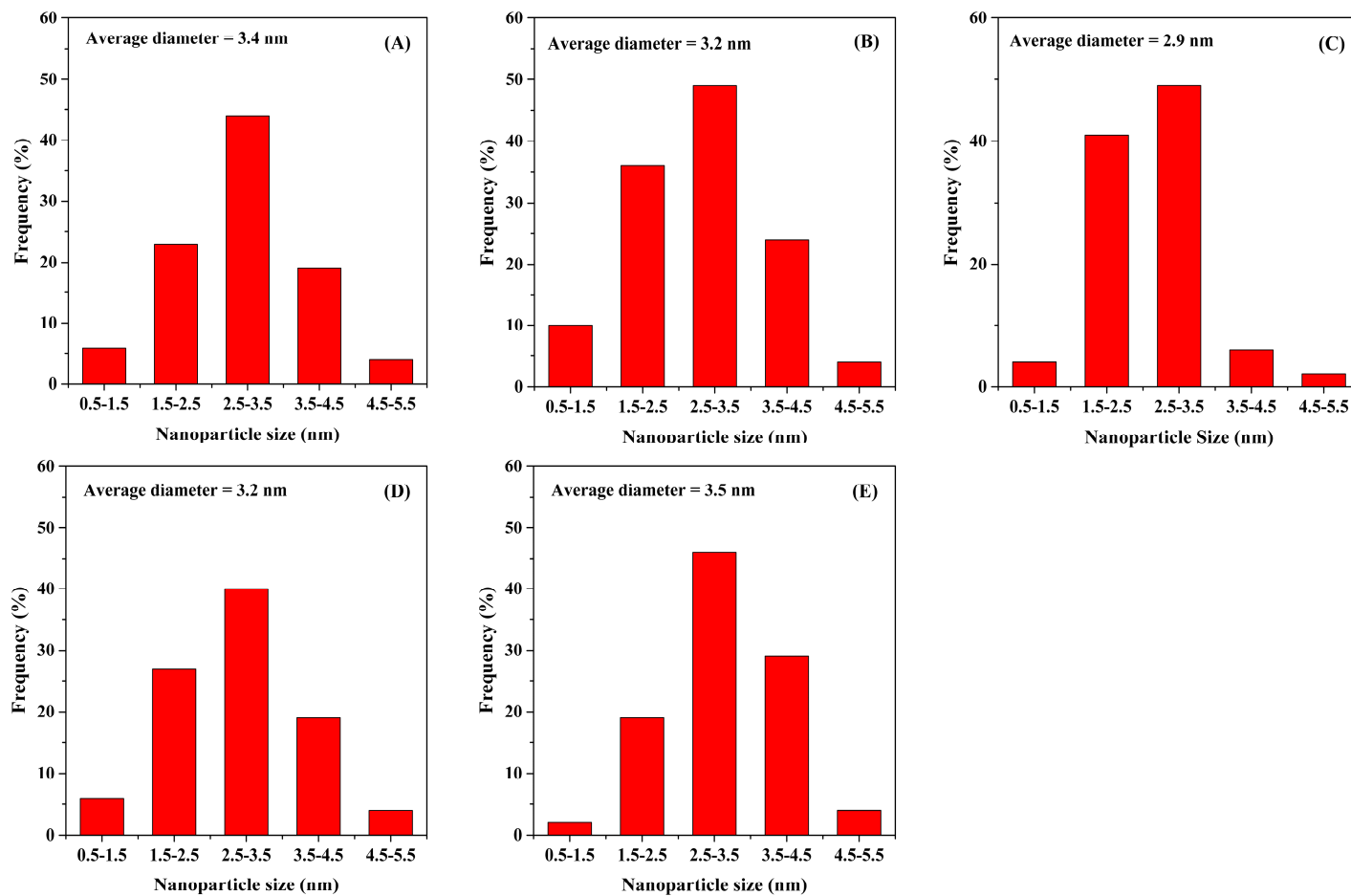


Figure S2. Noble metal particle-size distributions of (A) $0.89\text{Au}_{1.86}\text{Pd}/3\text{DOM TiO}_2$, (B) $0.87\text{Au}_{0.95}\text{Pd}/3\text{DOM TiO}_2$, (C) $0.91\text{Au}_{0.51}\text{Pd}/3\text{DOM TiO}_2$, (D) $0.89\text{Pd}/3\text{DOM TiO}_2$, and (E) $0.93\text{Au}/3\text{DOM TiO}_2$.

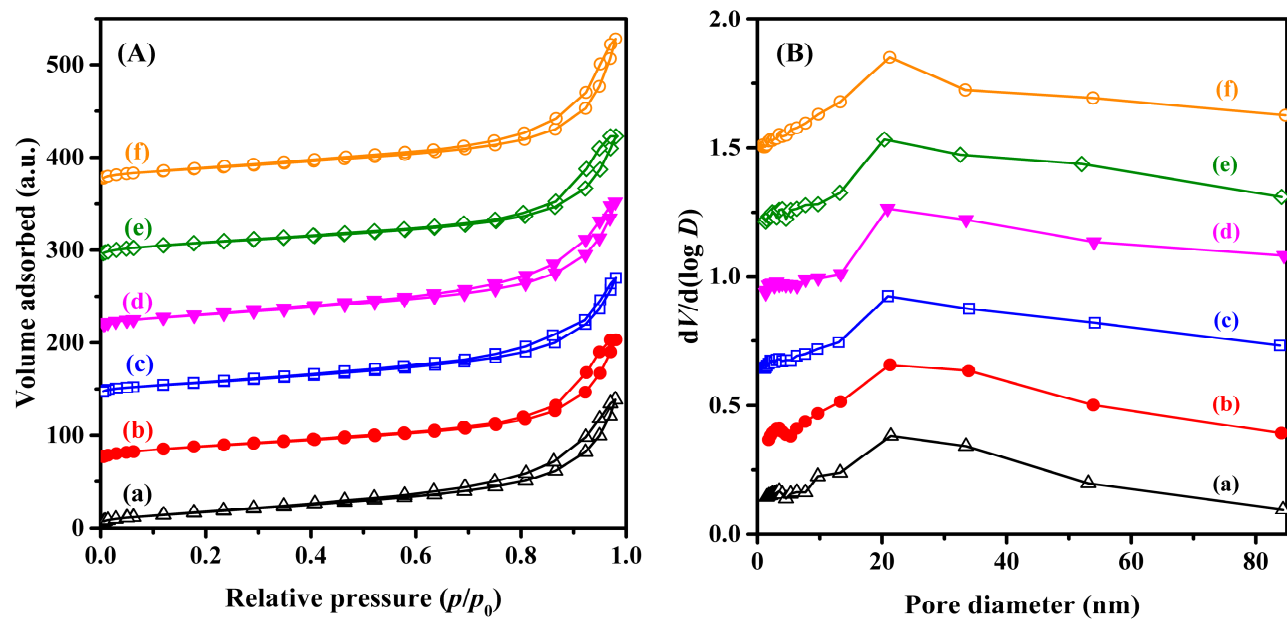


Figure S3. (A) N₂ adsorption–desorption isotherms and (B) pore-size distributions of (a) 3DOM TiO₂, (b) 0.89Au_{1.86}Pd/3DOM TiO₂, (c) 0.87Au_{0.95}Pd/3DOM TiO₂, (d) 0.91Au_{0.51}Pd/3DOM TiO₂, (e) 0.93Au/3DOM TiO₂, and (f) 0.89Pd/3DOM TiO₂.

Table S1. Data obtained by the curve-fitting of the XPS spectra of the samples.

Sample	Start BE	Peak BE	End BE	Height (CPS)	FWHM (eV)	Area (P) (CPS eV)	Area (N) KE ^{0.6}	At.%	F	Q	SF Al Scof	TXFN	BG	PP Height (CPS)	PP Height (N)	PP At.%
3DOM TiO₂																
Ti 2p	468.81	458.38	454.86	58844.39	1.04	103664.66	0.17	15.47		1	7.91	1182.52	Smart	60627.55	0.04	16.959
O 1s	536.46	529.59	526.56	64930.26	1.19	105530.09	0.68	43.189		1	2.93	1215.27	Smart	66260.44	0.09	38.124
0.93Au/3DOM TiO₂																
Au 4f	90.36	83.97	80.56	16666.39	0.98	34856.99	0.01	1.978		1	17.12	1039.29	Smart	16952.8	0.01	2.958
Ti 2p	468.63	458.40	455.01	38549.79	1.15	76451.31	0.13	10.309		1	7.91	1182.59	Smart	40275.04	0.03	11.069
O 1s	536.60	529.62	526.86	43193.96	1.35	93517.95	0.73	34.582		1	2.93	1215.36	Smart	44055.39	0.06	24.904
0.89Pd/3DOM TiO₂																
Pd 3d5	347.60	337.22	329.51	4572.97	1.17	9846.47	0.01	0.538		1	16.04	1131.34	Smart	4978.69	0	0.673
Ti 2p	468.46	458.36	454.96	54460.76	1.05	98143.11	0.16	14.225		1	7.91	1182.48	Smart	56766.93	0.04	16.171
O 1s	536.51	529.45	526.61	109455.92	1.05	183564.95	0.84	57.027		1	2.93	1215.48	Smart	113322.23	0.16	65.363
0.89Au_{1.86}Pd/3DOM TiO₂																
Au 4f	90.47	84.11	80.44	4853	1.11	11770.09	0.01	0.601		1	17.12	1039.34	Smart	5190.33	0	0.75
Pd 3d5	347.51	337.62	329.61	2060.42	2.17	4750.91	0.01	0.454	PF	1	9.48	1131.5	Smart	4189.1	0	1.132
Ti 2p	468.36	458.42	454.86	53640.76	1.04	97343.11	0.15	13.725		1	7.81	1178.56	Smart	58536.93	0.04	16.741
O 1s	535.36	529.96	527.36	83747.26	1.36	166701.17	0.76	53.541		1	2.93	1215.44	Smart	86469.85	0.12	58.904
0.87Au_{0.95}Pd/3DOM TiO₂																
Au 4f	90.31	84.03	81.16	5329.91	1.01	11397.21	0.01	0.61		1	17.12	1039.31	Smart	5444.35	0	0.767
Pd 3d5	347.56	337.24	329.66	3173.43	1.97	6836.43	0.01	0.684	PF	1	9.48	1131.35	Smart	4792.47	0	1.263
Ti 2p	468.81	458.38	454.86	57354.39	1.04	103064.66	0.16	15.27		1	7.81	1082.52	Smart	60527.55	0.04	16.651
O 1s	537.51	530.02	526.86	80657.38	1.26	154662.42	0.71	52.061		1	2.93	1215.47	Smart	83972.49	0.12	55.792
0.91Au_{0.51}Pd/3DOM TiO₂																
Au 4f	90.42	83.95	80.45	664.84	0.95	1521.12	0.01	0.1		1	16.12	1039	Smart	793.54	0	0.123
Pd 3d5	347.46	337.11	329.56	109.77	1.78	208.38	0.01	0.026	PF	1	9.18	1131.3	Smart	296.02	0	0.086
Ti 2p	468.50	458.3	454.26	58654.76	1.05	97943.11	0.15	14.345		1	7.86	1052.48	Smart	55743.93	0.04	16.101
O 1s	535.66	529.53	526.96	60429.65	1.2	97750.5	0.65	40.221		1	2.93	1215.24	Smart	61864.65	0.08	36.248

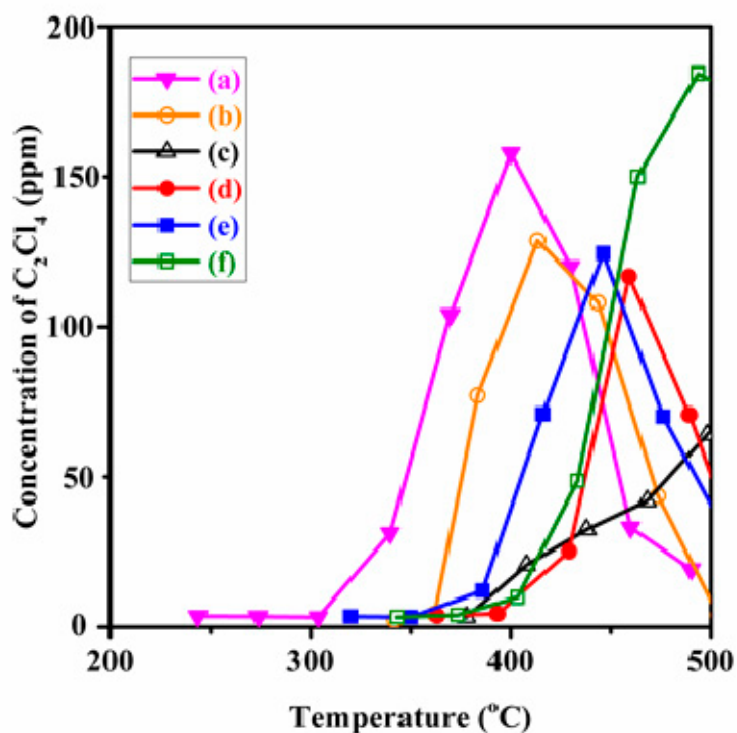


Figure S4. Concentrations of C_2Cl_4 formed over (a) $0.91Au_{0.51}Pd/3DOM TiO_2$, (b) $0.89Pd/3DOM TiO_2$, (c) $3DOM TiO_2$, (d) $0.89Au_{1.86}Pd/3DOM TiO_2$, (e) $0.87Au_{0.95}Pd/3DOM TiO_2$, and (f) $0.93Au/3DOM TiO_2$ at $SV = 20,000 mL/(g h)$.

Table S2. TCE oxidation rates over the $0.91Au_{0.51}Pd/3DOM TiO_2$ and various catalysts reported in the literature.

Catalyst	TCE concentration (ppm)	SV	Reaction rate at 250 °C (mol/(g _{cat} s))	Ref.
$0.91Au_{0.51}Pd/3DOM TiO_2$	750	20,000 mL/(g h)	2.69×10^{-7}	This work
CeMn-HT-N6A4	1000	15,000 h ⁻¹	1.12×10^{-7}	[36]
1.02 wt% Ru/TiO ₂ (P25)	500	60,000 mL/(g h)	1.13×10^{-7}	[37]
Ce _{0.15} Zr _{0.85} O ₂	1000	30,000 h ⁻¹	2.67×10^{-8}	[38]
LaMn _{1.2} O ₃	1000	15,000 h ⁻¹	4.08×10^{-8}	[33]
4Ce1Cr-(NH ₄) ₂ CO ₃	1000	15,000 h ⁻¹	4.31×10^{-8}	[39]
3.5 wt% VO _x /TiO ₂ -SG	1000	15,000 h ⁻¹	9.76×10^{-8}	[40]
4.3 wt% Mn/H-ZSM-5	1000	15,000 h ⁻¹	2.67×10^{-9}	[41]
0.42 wt% Pd/Al ₂ O ₃	1000	15,000 h ⁻¹	3.49×10^{-9}	[42]
CoFeAlO _x	1000	15,000 h ⁻¹	7.05×10^{-9}	[43]